

CHAPTER IV
RESULTS AND DISCUSSION



4.1 Simulation Results

The modeling results of the designed geometry with the MCNP4C program are shown in Table 4.1, along with the relationship between void fraction and scattered neutron count rate.

Table 4.1 The simulation results

Void fraction	Average density of mixture (g/cm ³)	Neutron Flux (particle/cm ²)			Relative %Error*
		Total	Uncollided	Scattered	
0.0	0.78401	0.0405422	0.0316515	0.0088907	0.86
0.1	0.70797	0.0402237	0.0321955	0.0080282	0.44
0.2	0.63194	0.0404711	0.0327518	0.0077193	0.88
0.3	0.55591	0.0401551	0.0333207	0.0068344	0.36
0.4	0.47988	0.0405079	0.0339026	0.0066053	0.69
0.5	0.40385	0.0399724	0.0344980	0.0054744	0.30
0.6	0.32782	0.0398034	0.0351072	0.0046962	0.22
0.7	0.25179	0.0399225	0.0357306	0.0041919	0.28
0.8	0.17575	0.0399601	0.0363688	0.0035913	0.19
0.9	0.09972	0.0399667	0.0370221	0.0029446	0.13
1.0	0.02369	0.0399411	0.0376910	0.0022501	0.05

* Estimated relative error is defined to be one estimated standard deviation of the mean $S\bar{x}$ divided by the estimated mean \bar{x} .

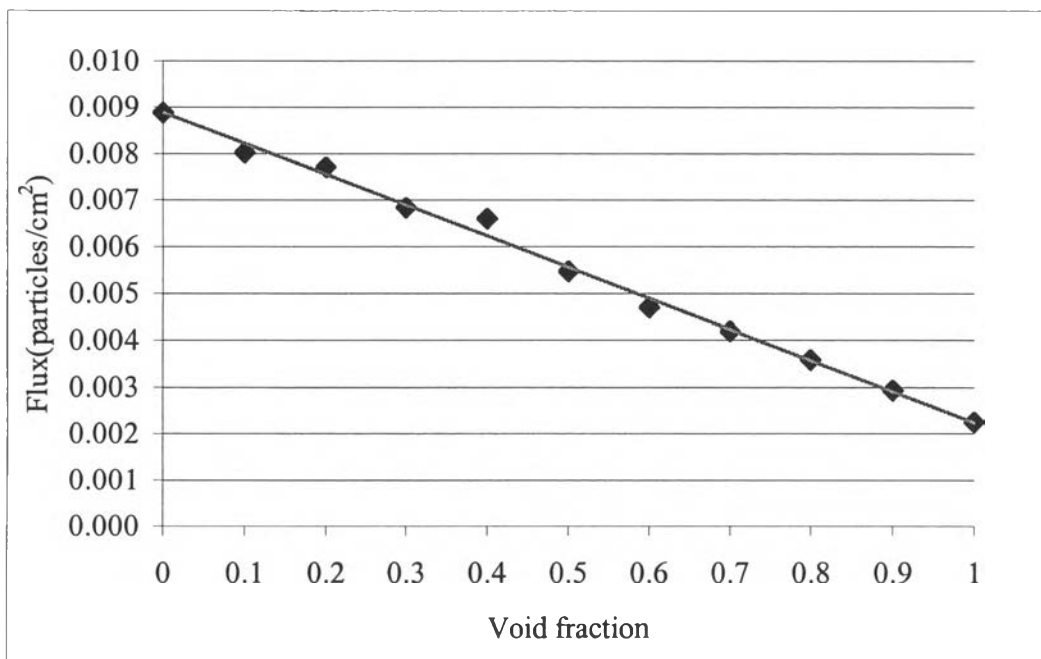


Figure 4.1 The relationship between scattered neutron flux and void fraction.

The density of the mixture was varied in the range of 0 to 1 void fraction. The total neutron flux and uncollided neutron flux were estimated from the MCNP4C program. In order to evaluate the scattered neutron flux, the uncollided flux was subtracted from the total neutron flux. As suggested in the program manual, the relative error for a point detector should be reliable when the value is less than 0.05.

The contrast ratio (Eq. 2.1) is a parameter that can be used to indicate the performance of the neutron scattering technique. From Table 4.1, the average contrast ratio is 2.95, which is comparable with a previous work (Hussein and Han, 1995).

The relationship between the void fraction and scattered neutron flux in Figure 4.1 shows that, as the void fraction decreases, the scattered neutron count rate increases. This is because of the diminishing of the liquid fraction. The concentration of hydrogen atoms in the liquid phase is higher than in vapor phase; therefore, the number of scattered neutrons mostly come from the collision with hydrogen atoms in liquid phase. Consequently, the scattered neutrons are proportional to the liquid fraction. Furthermore, linearity is achieved over the whole range of void fraction,

facilitating the calibration process. The feasibility of this scatterometer design has, therefore, been demonstrated.

4.2 Static Experiment Results

The results from the static experiments are shown in Figure 4.2. The raw data can be found in Appendix B. The estimated lucite fraction was calculated from equation (2.2). Table 4.2 reports the mean count rate of neutron for each lucite fraction. Each fraction is an average of ten experiments. The figure shows that the linear response was achieved. Thus, there is a possibility to predict water fraction or void fraction by using this design neutron scattering device. Therefore, the dynamic experiment can be continued.

Table 4.2 The mean of neutron count rate for various lucite fraction

Lucite fraction	Mean count rate for 2 minutes	% Stand deviation
0	1731.3	0.76
0.09	1744.1	0.73
0.17	1747.4	0.76
0.26	1763.9	0.75
0.35	1769.0	0.75
0.43	1777.5	0.75
0.52	1798.6	0.75
0.60	1819.9	0.74
1.00	1853.7	0.73

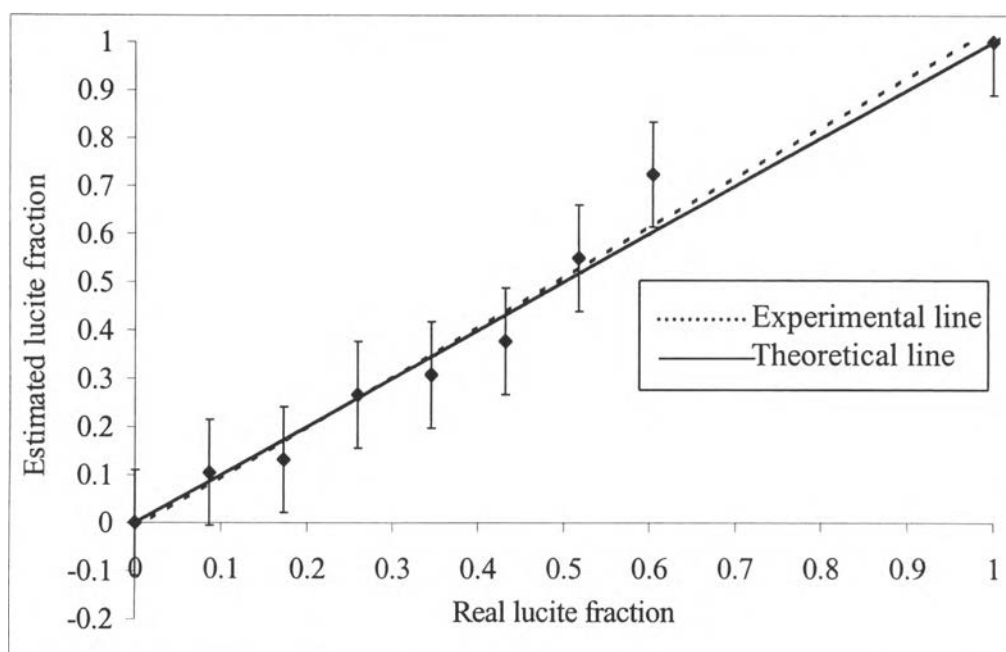


Figure 4.2 The correlation between estimated void fraction and real lucite fraction of static experiment.

The contrast ratio of the static experiment calculated from (2.1), 0.71, is smaller than the simulation results, which means that the background rate (signal of empty test section) is higher. Since in the real experiment, there are many factors affecting the higher background count rate such as electronic noise, external noise and high epi-cadmium signal (above 0.5 eV) etc. Even though electronic noise was eliminated by selecting the multichannel analyzer, not all signals generated by the surroundings of work site were eliminated.

Also, this experiment used the cadmium sheet to eliminate neutrons of energy below the cadmium cut-off of 0.5 eV but it did not get rid of the higher energy produced from outside which may cause the high background count rate. However, the epi-cadmium signal can be reduced by using a detector with lower efficiency at detecting high-energy neutrons but still good for low energy neutrons such as a BF_3 detector.

4.3 Dynamic Experiment Results

Table 4.3 shows the count rate for the counting period of 12 seconds at different density values, extracted from a steam table. The correlation between the density of compressed water and the count rate shows the linear relationship, as seen in Figure 4.3. The raw data can be found in Appendix C. As the density increased, the count rate increased. It was compatible with the fact that at higher density, the number of hydrogen atoms per unit volume is higher; therefore, the probability of neutron interaction is higher.

Table 4.3 The count rate for 12 seconds at different density values

Density of Compressed water	Count rate for 12 second
989.81	1.79×10^5
960.71	1.66×10^5
919.29	1.48×10^5
867.38	1.33×10^5

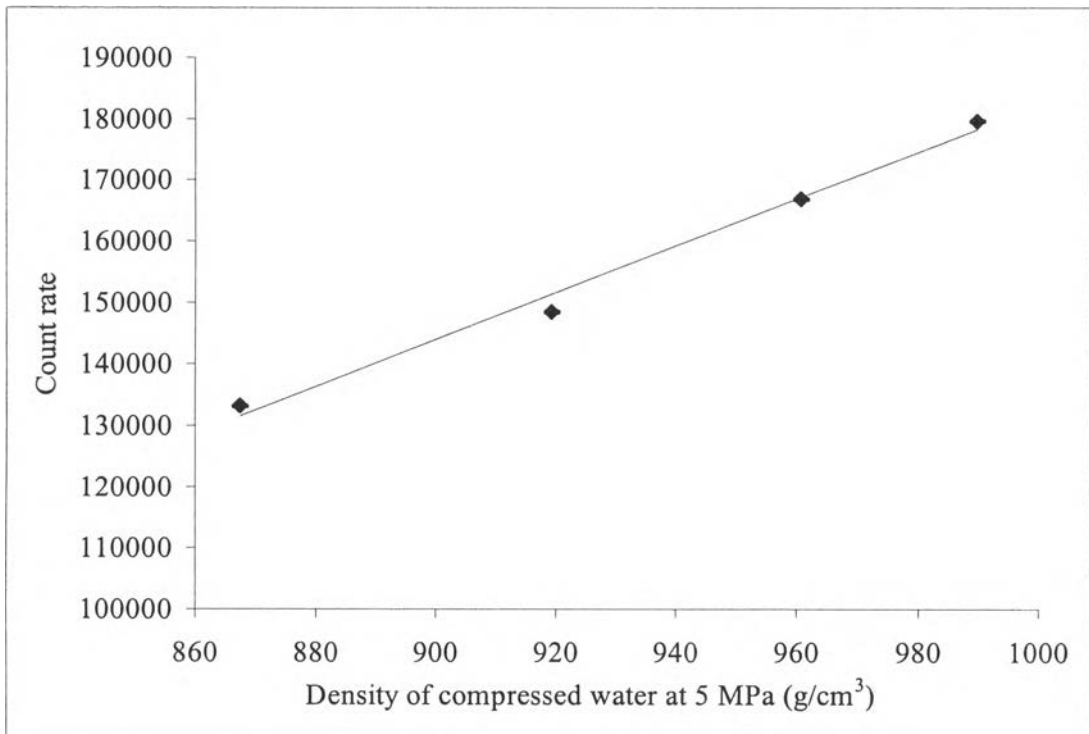


Figure 4.3 The relationship between count rate and density of compressed liquid.